Electronic Supplementary Material (ESI) for Journal of Materials Chemistry A.
This journal is © The Royal Society of Chemistry 2019

Supporting Information

Nitrogen-Rich Carbon-Onion-Constructed Nanosheets: An Ultrafast and Ultrastable Dual Anode Material for Sodium and Potassium Storage

Sitong Liu, Beibei Yang, Jisheng Zhou, and Huaihe Song**

Dr. S. T. Liu, B. B. Y, Prof. J. S. Zhou, Prof. H. H. Song
Beijing Advanced Innovation Center for Soft Matter Science and Engineering, State Key Laboratory of Chemical Resource Engineering, Beijing Key Laboratory of Electrochemical Process and Technology for Materials, Beijing University of Chemical Technology, Beijing 100029, P. R. China

*E-mail: zhoujs@mail.buct.edu.cn; songhh@mail.buct.edu.cn

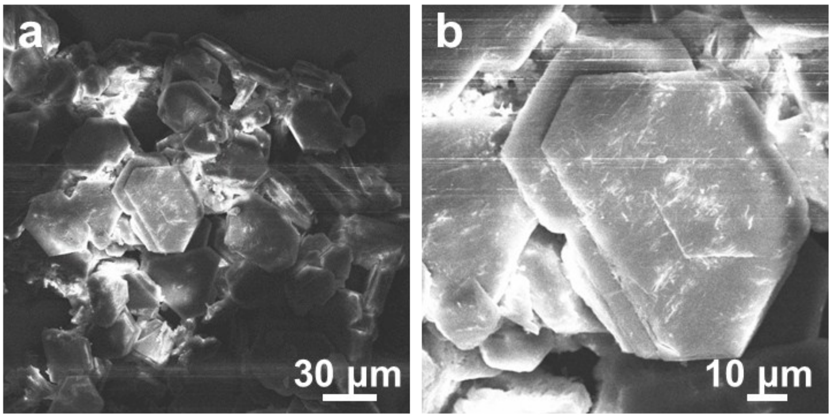

Fig. S1 (a,b) SEM images of bulk microplate of Co-HMT frameworks.

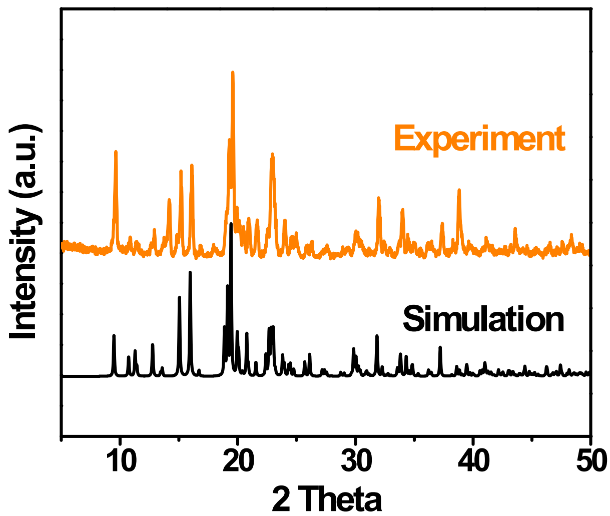

Fig. S2 Experimental powder and simulated XRD patterns of layered Co-HMT frameworks.

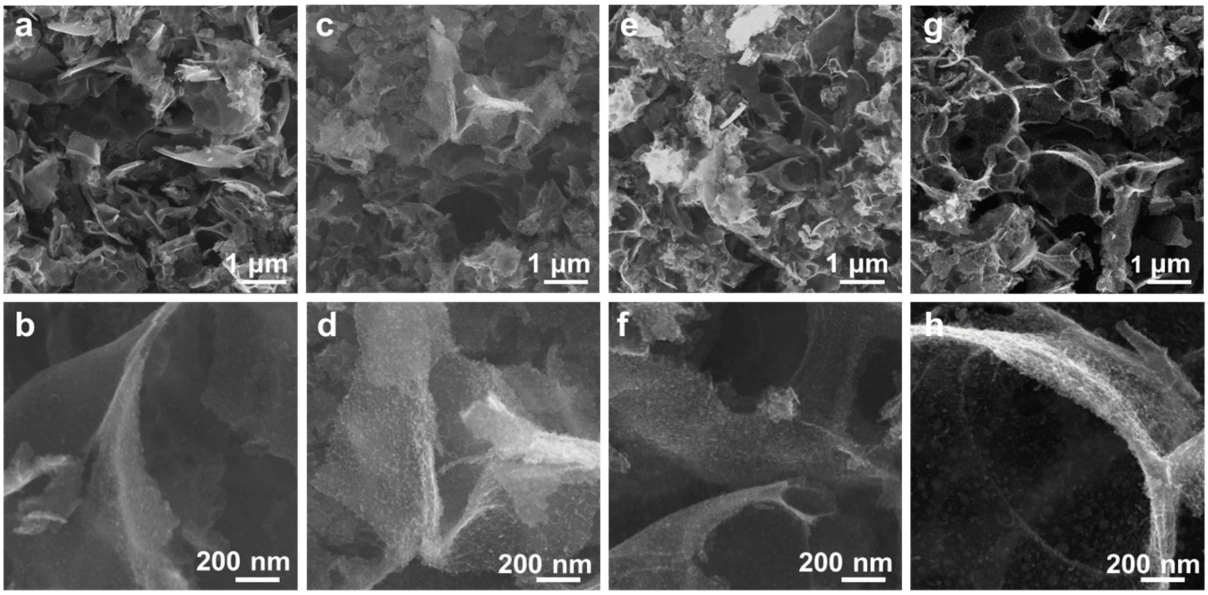

Fig. S3 SEM images of N-rich carbon/Co composite nanosheets obtained at different pyrolysis temperature of (a,b) 500, (c,d) 600, (e,f) 700 and (g,h) 800 ^{o}C, respectively.

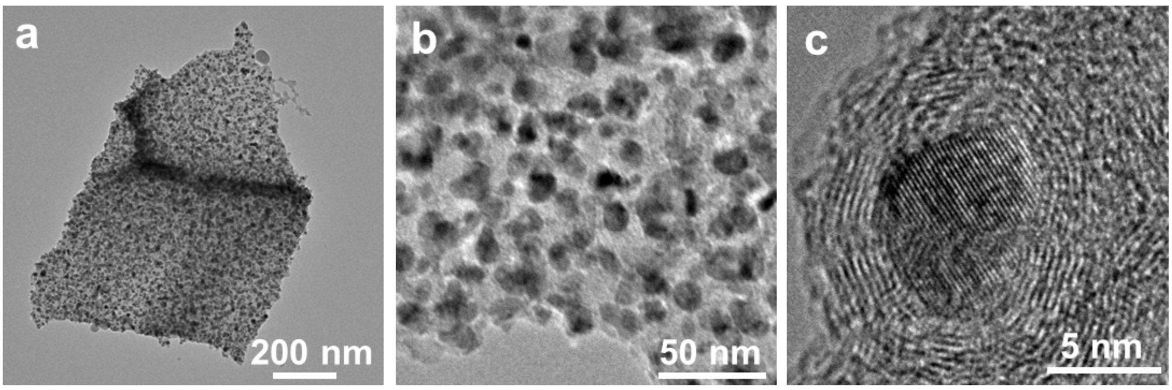

Fig. S4 (a,b) TEM images and (c) HRTEM of N-rich carbon/Co composite composite nanosheets pyrolyzed at 500 ^{o}C.

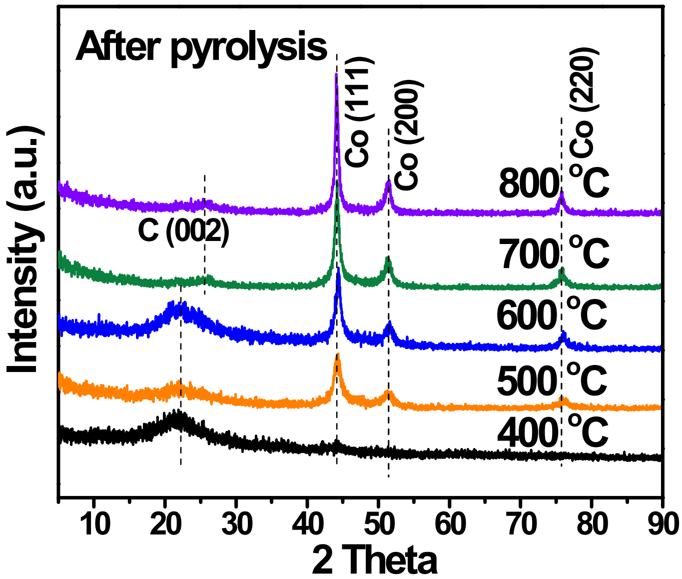

Fig. S5 XRD patterns of N-rich carbon/Co composite nanosheets obtained at different pyrolysis temperature.

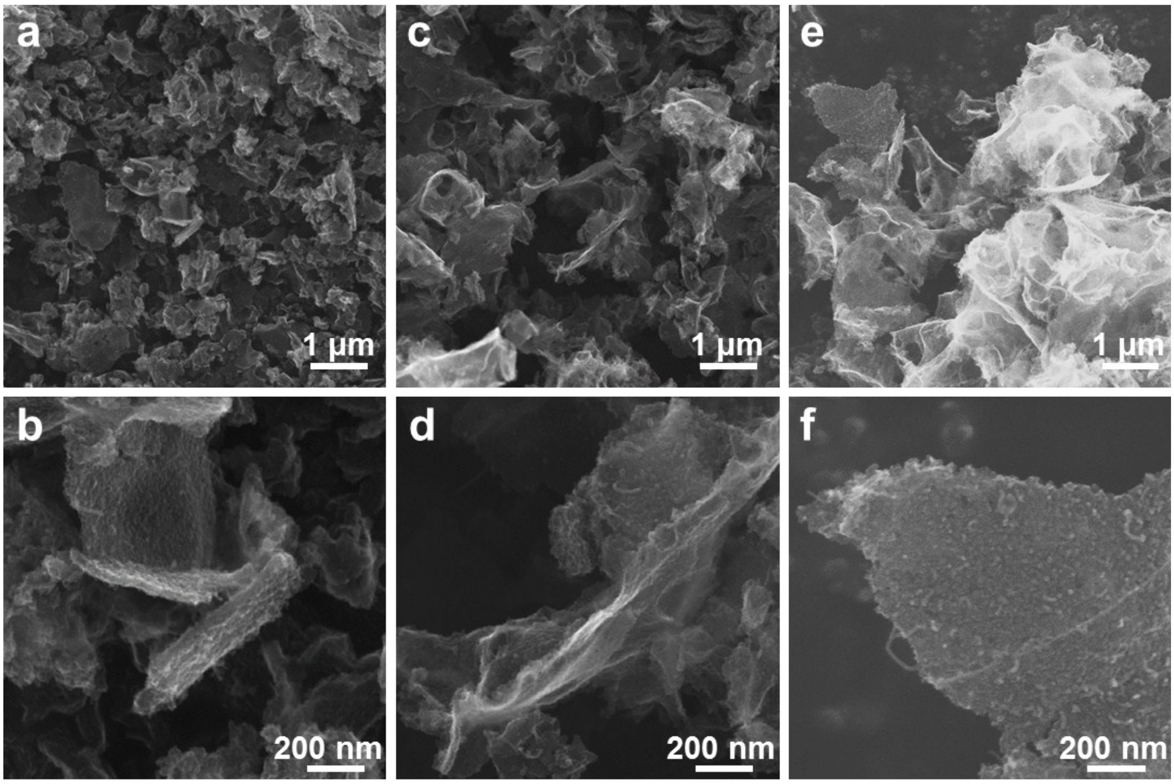

Fig. S6 SEM images of (a,b) HCONs-600, (c,d) HCONs-700, and (e,f) HCONs-800, respectively.

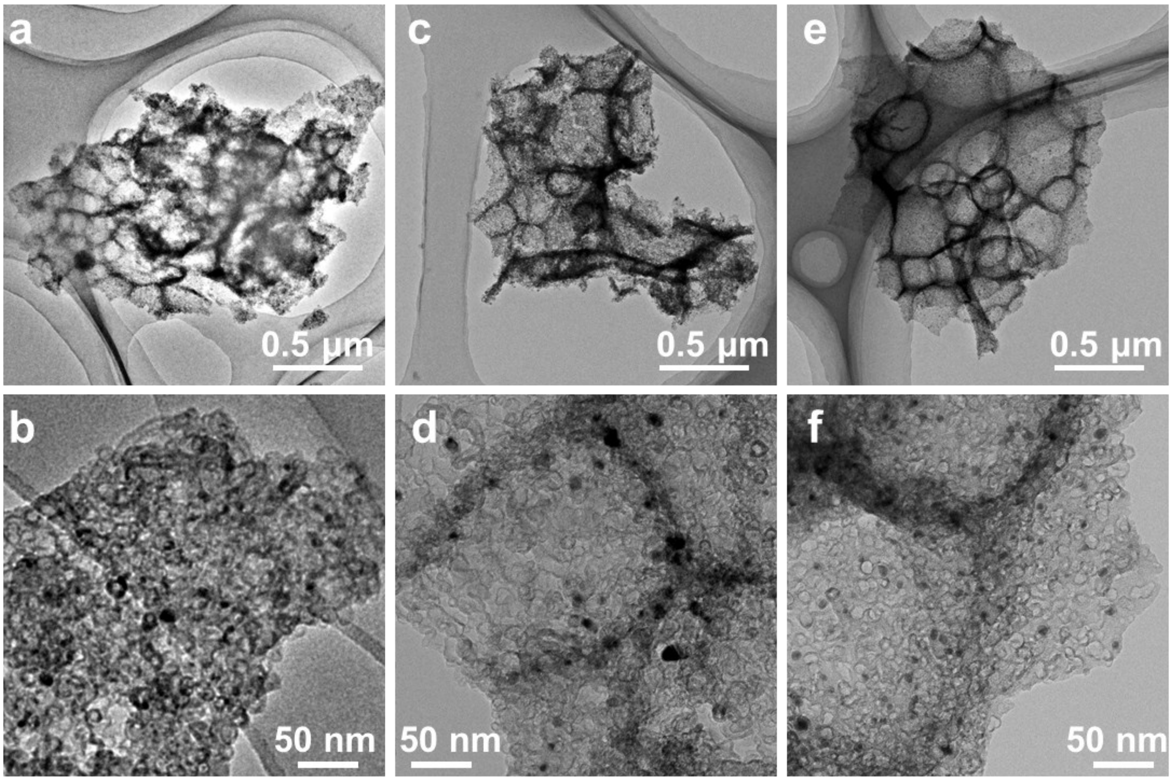

Fig. S7 TEM images of (a,b) HCONs-600, (c,d) HCONs-700, and (e,f) HCONs-800, respectively.

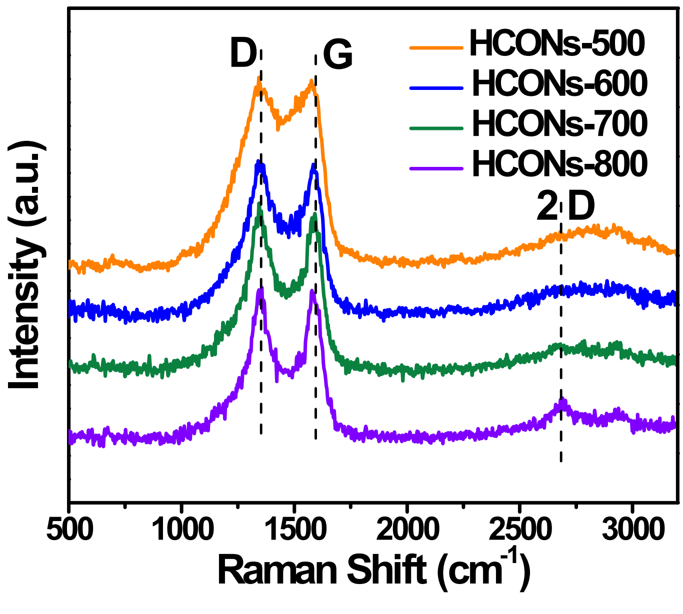

Fig. S8 Raman spectra of HCONs samples.

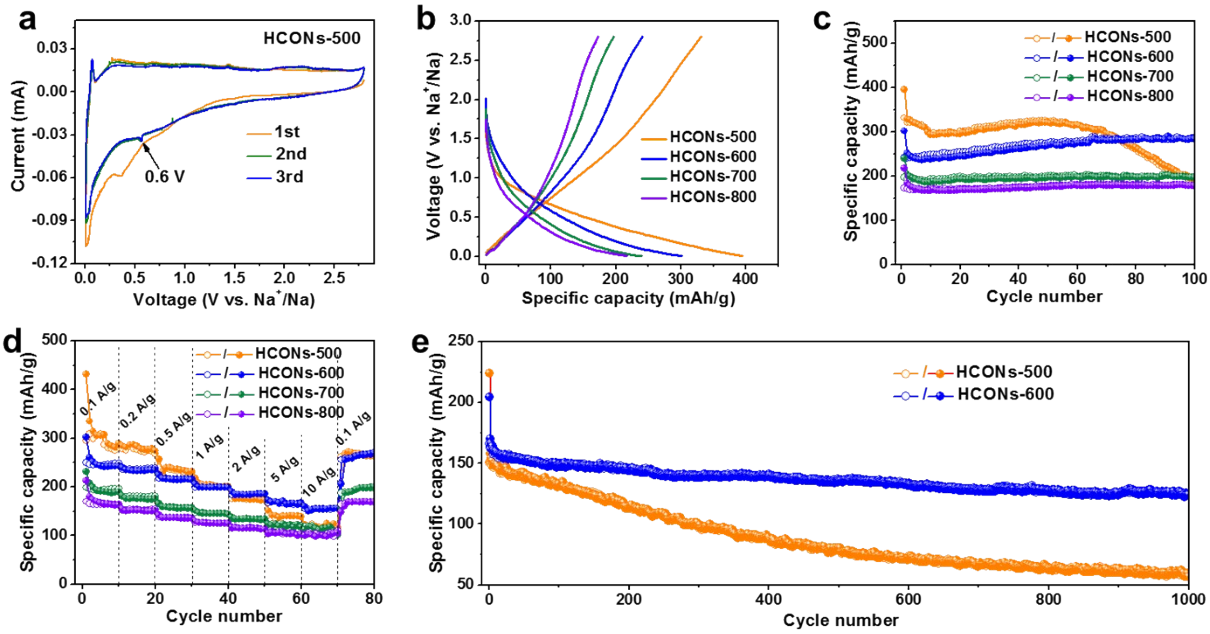

Fig. S9 Electrochemical sodium storage performance of HCONs in ether-based $NaCF_3SO_3$ electrolyte. (a) CV curves of HCONs-500 over a voltage range of 0.01-2.8 V at 0.1 mV s^{-1}; (b) voltage profiles of the first cycle for the HCONs electrodes at 0.1 A g^{-1}; (c) cycling performance at 0.1 A g^{-1}; (d) rate capability; (e) long-term cycling performance of HCONs-500 and HCONs-600 at 5 A g^{-1}.

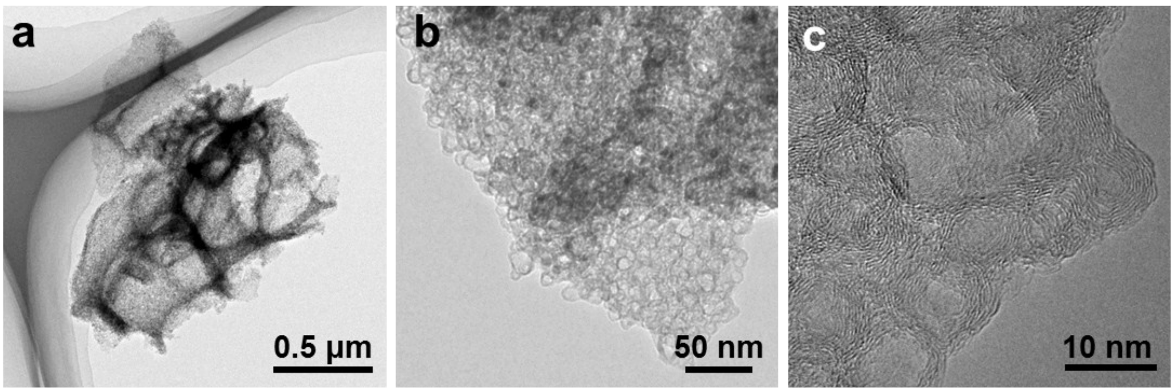

Fig. S10 (a,b) TEM and (c) HRTEM images HCONs-500 electrode after 10000 cycles at 5 A^{-1} in $NaClO_4$ ester-based electrolyte.

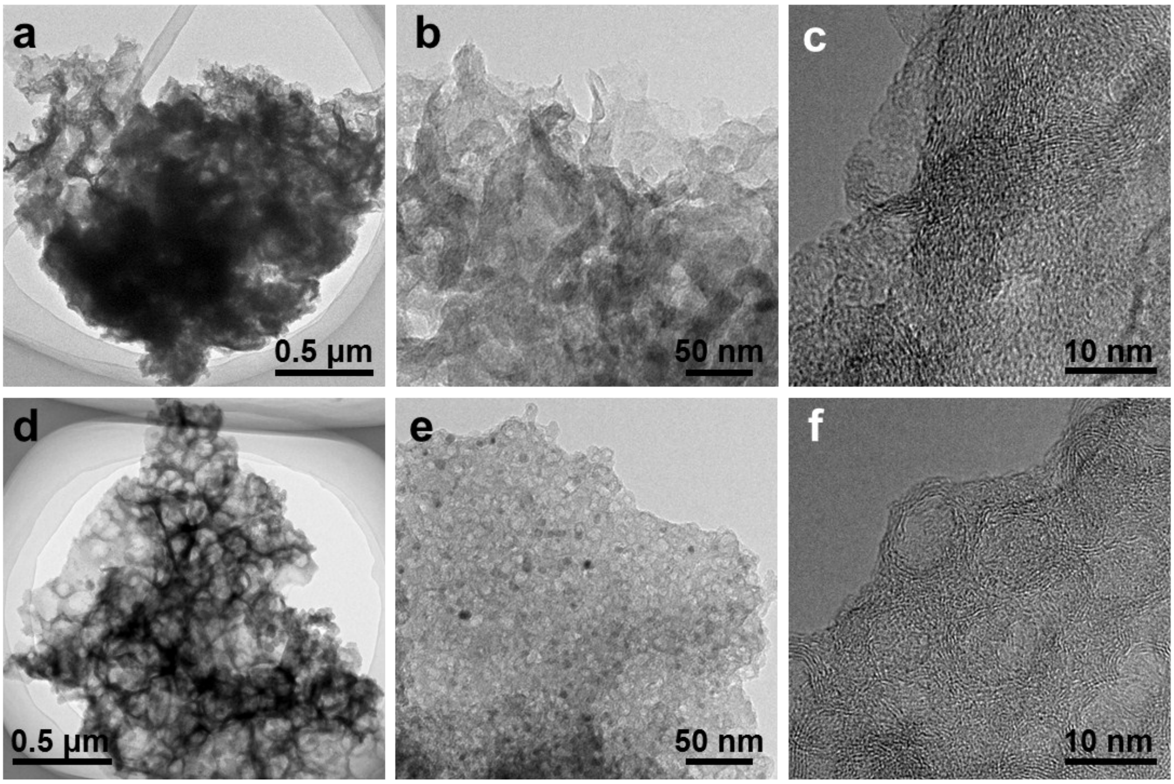

Fig. S11 (a,b) TEM and (c) HRTEM images HCONs-500 electrode after 1000 cycles at 5 A^{-1} in $NaCF_3SO_3$ ether-based electrolyte; (d,e) TEM and (c) HRTEM images HCONs-600 electrode after 1000 cycles at 5 A^{-1} in $NaCF_3SO_3$ ether-based electrolyte.

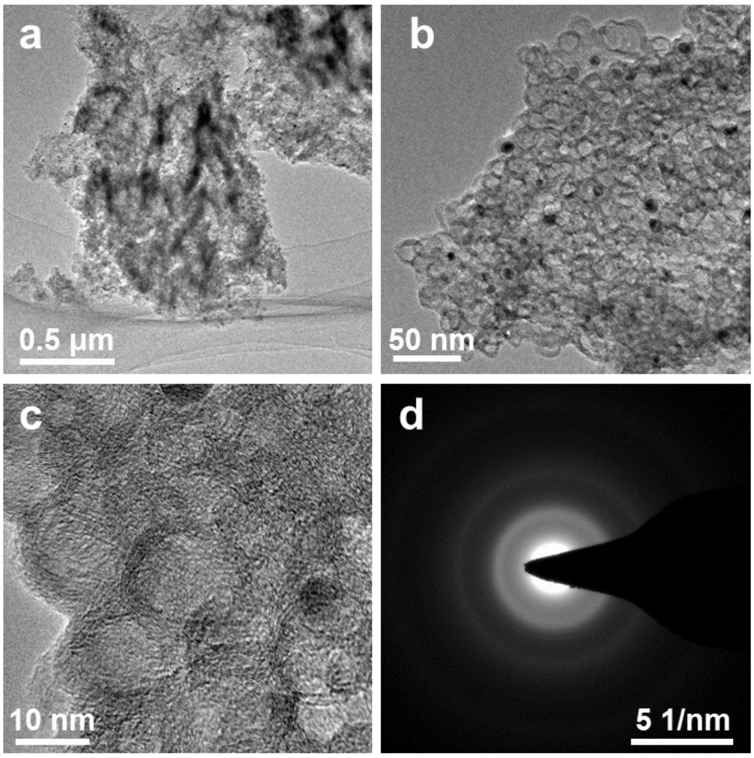

Fig. S12 (a,b) TEM and (c) HRTEM images of HCONs-500 electrode after 5000 cycles at 2 A g^{-1} in KPF_6 electrolyte; (d) the corresponding SAED pattern.

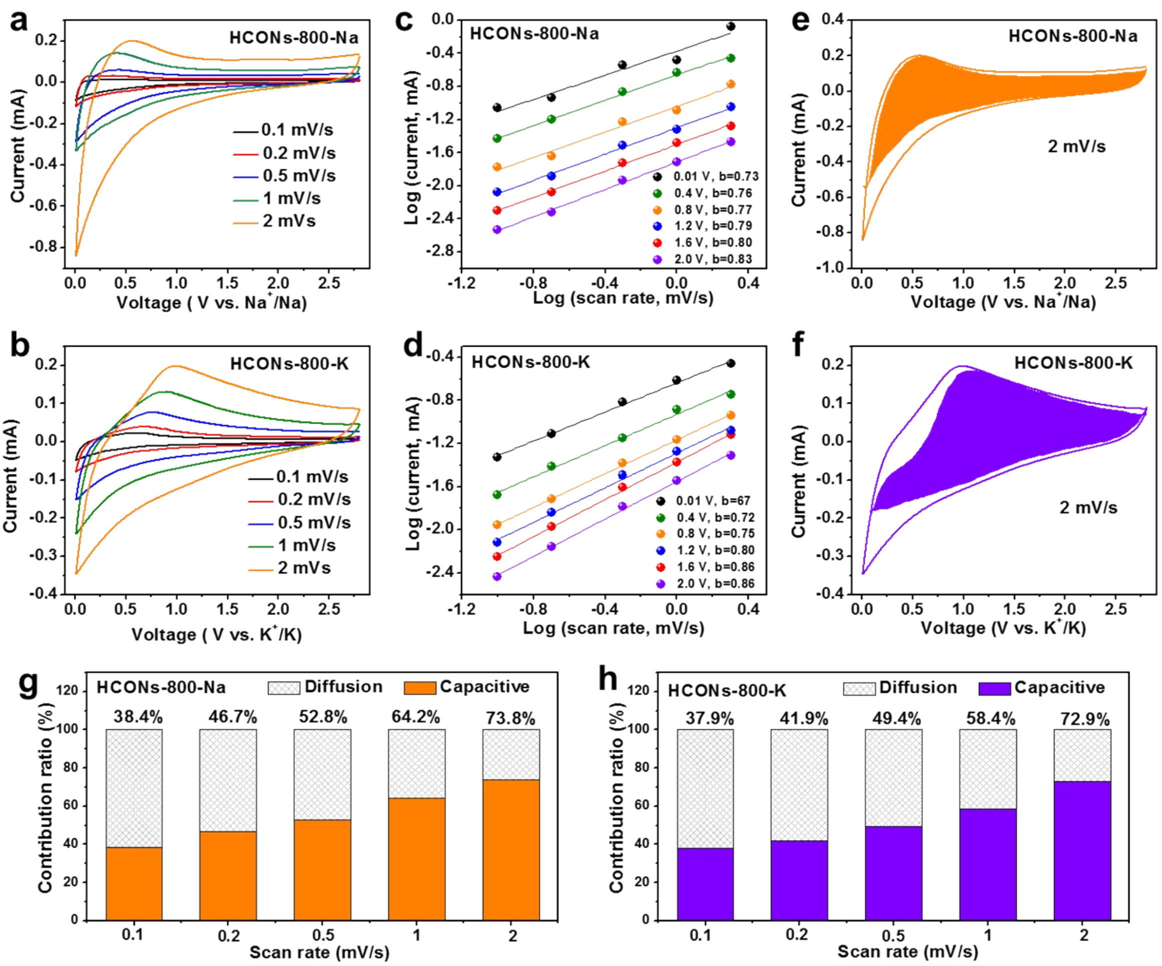

Fig. S13 Electrochemical kinetic analysis of HCONs-800 electrode in SIBs and KIBs. a,b) CV curves at different scan rates; c,d) linear relationships between the log(i) and log(v); e,f) separation of the capacitive contribution in SIBs and KIBs at a scan rate of 2 mV s^{-1}; g,h) contribution ratio of the capacitive and diffusion-controlled charge at different scan rates.

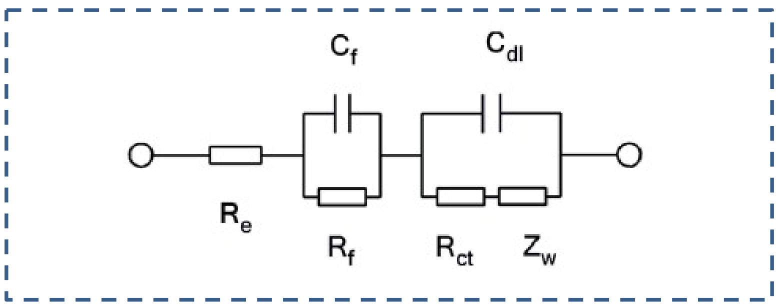

Fig. S14 Randles equivalent circuit for the electrodes.

Supplementary Note: The diffusion coefficient (*D*) in HCONs electrodes can be calculated from the GITT potential profiles by Fick's second law with the following Equation S1:

$$D = \frac{4}{\pi\tau}\left(\frac{m_B V_M}{M_B S}\right)^2\left(\frac{\Delta E_S}{\Delta E_\tau}\right)^2 \quad (1)$$

where τ is the current pulse time; m_B is the electrode active material mass; *S* is the geometric area of the electrode; ΔE_S is the quasi-thermodynamic equilibrium potential difference before and after the current pulse; ΔE_τ is the potential difference during current pulse; V_M is the molar volume of the HCONs; M_B is the molar mass of carbon. The value of M_B/V_M can be obtained from the density of HCONs samples.

The density of HCONs can be calculated according to the following Equation S2:

$$\rho = \frac{1}{V_{total} + \frac{1}{\rho_{Carbon}}} \quad (2)$$

where ρ (g cm^{-3}) is the density of HCONs, V_{total} (cm^3 g^{-1}) is the total pore volume measured according to nitrogen adsorption-desorption isotherms, ρ_{Carbon} is the true density of carbon (2 g cm^{-3}). In this work, the V_{total} of HCONs-500 and HCONs-800 is 0.337 and 0.757 cm^3 g^{-1}. Thus, the densities of HCONs-500 and HCONs-800 are calculated to be 1.19 and 0.80 g cm^{-3}, respectively.

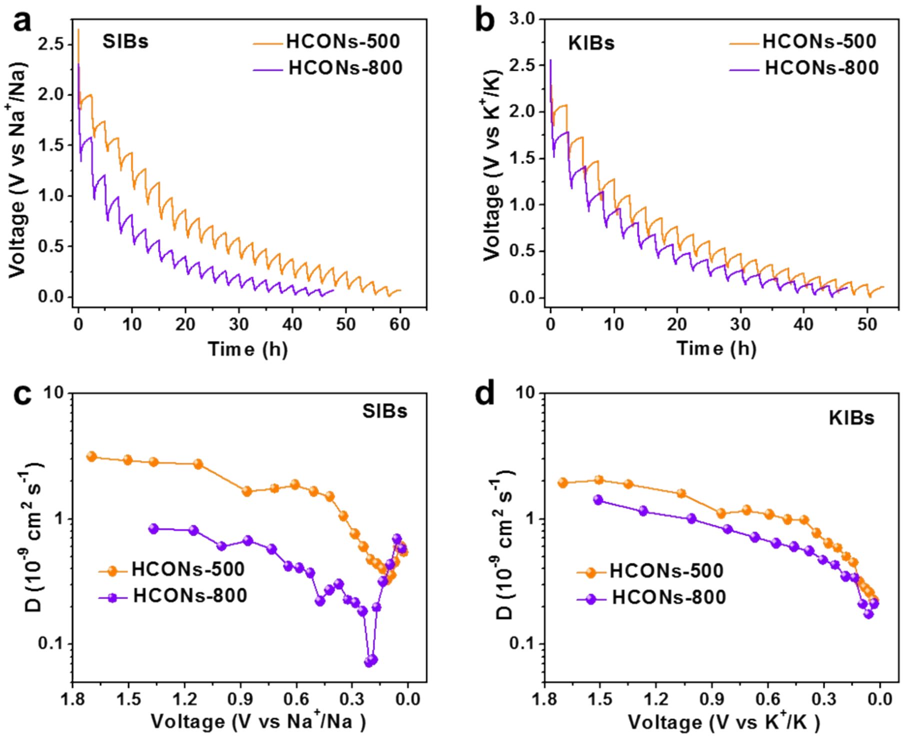

Fig. S15 GITT potential profiles for a) HCONs-500 and b) HCONs-800 of discharge process in SIBs and KIBs, respectively; the corresponding diffusion coefficients in c) SIBs and d) KIBs calculated from GITT potential profiles.

Table S1. Structural parameters of HCONs samples.

Sample	d_{002} (nm)	L_c (nm)	I_D/I_G	S_{BET} ($m^2\ g^{-1}$)	S_{micro} ($m^2\ g^{-1}$)	S_{meso} ($m^2\ g^{-1}$)	V_{total} ($cm^3\ g^{-1}$)	V_{micro} ($cm^3\ g^{-1}$)
HCONs-500	0.349	1.71	1.03	108.2	7.3	100.9	0.337	0.003
HCONs-600	0.347	1.92	1.07	270.9	33.8	237.1	0.615	0.017
HCONs-700	0.346	2.04	1.09	340.1	34.4	305.7	0.665	0.016
HCONs-800	0.344	2.24	1.05	354.6	19.6	335.0	0.757	0.008

Table S2. XPS results of elemental contents and doping levels of N-6, N-5, N-Q and N-O in the HCONs samples.

Sample	XPS (at%)			N-6 (%)	N-5 (%)	N-Q (%)	N-O (%)
	C	N	O				
HCONs-500	76.42	16.54	5.82	59.11	16.95	17.96	5.97
HCONs-600	83.84	9.10	5.95	52.44	12.16	24.18	11.21
HCONs-700	88.32	5.68	5.23	49.39	7.05	30.54	13.01
HCONs-800	87.58	3.57	8.50	46.49	4.25	35.20	14.06

Table S3. Comparison of the electrochemical performance of various carbonaceous materials as anodes for SIBs in ester-based electrolyte.

Sample	Specific capacity (mAh g^{-1}) /Current density (A g^{-1})	Long-term cycle stability (mAh g^{-1}) /Current density (A g^{-1})/Cycle number	Initial coulombic efficiency (%)	Ref.
N-doped porous carbon nanosheets	323/0.1 140/0.5 89/1 50/20	155/0.05/260	34.9	[S1]
3D amorphous carbon	280/0.03 205/0.3 138/1.2 81/4.8 66/9.6	188/0.3/600	75	[S2]
Mesoporous soft carbon	193/0.1 105/1 90/2 62/5 53/10	105/0.5/3000	45	[S3]
Bamboo-like carbon nanotubes	271/0.05 167/0.1 138/0.2 104/0.5 81/1	104/0.5/160	30	[S4]
Nitrogen-rich mesoporous carbon	210/0.1 118/0.5 86/1 49/2	111/0.5/800	54.2	[S5]
Carbon quantum dots	356/0.1 290/0.2 166/2 130/5 104/10	150/2.5/3000 100/5/10000	34.8	[S6]
S-doped N-rich carbon nanosheets	300/0.1 220/1 190/2 150/5 110/10	211/1/1000	43.9	[S7]
Carbon nanosheet frameworks	203/0.5 150/1 106/2 66/5	255/0.1/210	57.5	[S8]
Hierarchical N/S-codoped carbon	210/0.1 180/0.2 155/0.5 143/1 130/2.5 131/5 130/10	150/0.5/3400	26.7	[S9]
HCONs-500	293/0.1 256/0.2 225/0.5 196/1 168/2 146/5 131/10	151/5/10000	45	This work

Table S4. Comparison of the electrochemical performance of various carbonaceous materials as anodes for SIBs in ether-based electrolyte.

Sample	Specific capacity (mAh g^{-1}) /Current density (A g^{-1})	Long-term cycle stability (mAh g^{-1}) /Current density (A g^{-1})/Cycle number	Initial coulombic efficiency (%)	Ref.
Graphite	116/0.2 102/10	110/0.2/6000	92	[S10]
Carbon nanotubes	212/0.1 193/0.2 171/0.5 155/1 140/2 132/5	185/0.1/100 106/2/1000 96/5/100	83.4	[S11]
Hard carbon	320/0.1C 217/3C 1C = 30 mA g^{-1}	250/0.5C/100 75/7C/2000	63	[S12]
Reduced graphene oxide	625/0.1 332/1 199/5	509/0.1/100 250/1/1000	74.6	[S13]
High N-doped carbon	254/0.1 212/0.2 188/0.5 175/1 160/2 142/5 112/10	145/2/500 123/5/500 95/10/500	58	[S14]
Carbon black	234/0.05 196/0.1 170/0.2 133/0.8 120/1.6 105/3.2	196/0.05/100 72/3.2/2000	61.45	[S15]
N-doped expanded graphone oxide	300/0.1 250/0.5 221/1 201/2 189/5 175/10 150/20	120/10/5000	72.08	[S16]
Carbon nanofiber films	449/0.05 205/1 170/2 148/5 121/10	178/1/500 151/2/500 126/5/500 111/10/500	85.8	[S17]
HCONs-500	250/0.1 236/0.2 217/0.5 199/1 184/2 167/5 154/10	124/5/1000	84	This work

Table S5. Comparison of the reversible capacities of typical carbonaceous materials as anodes for SIBs in ester-based electrolyte and in ether-based electrolyte.

Sample	**Ester-based electrolyte** **Specific capacity (mAh g^{-1}) /Current density (A g^{-1})**	**Ether-based electrolyte** **Specific capacity (mAh g^{-1}) /Current density (A g^{-1})**	**Ref.**
Graphite	150/0.1	Negligible electrochemical activity	[S18]
Reduced graphene oxide	**262/0.1**	**509/0.1** 199/5	[S13]
Carbon nanotubes	178/0.2 147/0.5 122/1 97/2 69/5	193/0.2 171/0.5 155/1 140/2 132/5	[S11]
Carbon black	**107/0.05**	**234/0.05** 196/0.1 170/0.2 133/0.8 120/1.6 105/3.2	[S15]
Hard carbon	280/1C (1C = 30 mA g^{-1}) **61/3C**	320/0.1C **217/3C**	[S12]
HCONs-500	293/0.1 256/0.2 225/0.5 196/1 168/2 146/5 131/10	295/0.1 276/0.2 235/0.5 204/1 175/2 141/5 120/10	This work

Tabel S6. Comparison of the electrochemical performance of various carbonaceous materials as anodes for KIBs.

Sample	Specific capacity (mAh g^{-1}) /Current density (A g^{-1} or 1C= 280 mA g^{-1})	Long-term cycle stability (mAh g^{-1}) /Current density (A g^{-1})/Cycle number	Initial coulombic efficiency (%)	Ref.
Graphite	264/0.1C 210/1C 185/2C 140/5C	151/2C/50	57.4	[S19]
Hierarchical porous carbon	240/0.05 214/0.1 202/0.2 181/0.5 164/1	168/0.2/100 156/0.5/500 158/1/2000	25	[S20]
N-doped carbon nanotubes	297/0.05 180/0.5 102/2	255/0.05/300 102/2/500	24.45	[S21]
Mesoporous carbon	286/0.05 255/0.1 219/0.2 186/0.5 144/1	198/0.2/200 186/0.5/200 160/1/200 147/1/1000	63.6	[S22]
S/O codoped porous hard carbon microspheres	230/0.05 213/0.2 176/0.5 158/1	227/0.05/100 101/0.2/200 173/0.5/200 133/1/200 108/1/2000	61.7	[S23]
Commercial expanded graphite	263/0.01 242/0.02 219/0.05 205/0.1 175/0.2	174/0.2/500	81.56	[S24]
Actived carbon from graphite	209/0.1 159/0.2 114/0.4 72/0.8 30/1	100.3/0.2/100	—	[S25]
Yolk–shell carbon spheres	314/0.05 260/0.1 227/0.2 196/0.5 155/1 134/2 121/5	218/0.2/500 138/1200	53	[S26]
Chitin-derived natural nitrogen-doped carbon nanofibers	240.1/0.1C 211.3/0.2C 153.5/0.5C 123.8/1C 109.3/2C 84.7/5C	103.4/2C/500	37.8	[S27]
Soft carbon	264/C/10 210/1C 185/2C 140/5C	151/2C/50	56.4	[S19]
Hard carbon microspheres	262/0.1C 229/0.5C 205/1C 190/2C 136/5C	216/0.1C/100	61.8	[S28]

Hard-soft composite carbon	230/0.5C 210/1C 190/2C 121/5C 80/10C	160/1C/200	67	[S29]
N-doped graphene	350/0.05 200/0.1	210/0.1/100	52	[S30]
Highly N-doped carbon nanofibers	238/0.1 192/0.5 172/1 126/5 104/10	205/0.5/1000 164/1/2000 146/2/4000	49	[S31]
N/O-dual doped hard carbon	315/0.05 118/3	130/1.05/1100	25	[S32]
Hollow Carbon Architecture	340/0.1C	250/0.5C/150	72.1	[S33]
HCONs-500	311/0.1 257/0.2 232/0.5 197/1 168/2 136/5 105/10	132/2/5000	34	This work

Tabel S7. Fitting results of the EIS curves in Fig. S14 using the equivalent circuit.

Samples	**SIBs**			**KIBs**		
	R_e (Ω)	**R_f (Ω)**	**R_{ct} (Ω)**	**R_e (Ω)**	**R_f (Ω)**	**R_{ct} (Ω)**
HCONs-500	9.21	7.82	8.02	11.23	30.78	34.68
HCONs-600	9.32	8.34	9.15	11.40	40.21	41.34
HCONs-700	9.46	21.21	18.76	11.78	40.79	44.79
HCONs-800	9.17	20.20	19.34	11.91	86.64	98.76

References

1 H. G. Wang, Z. Wu, F. L. Meng, D. L. Ma, X. L. Huang, L. M. Wang and X. B. Zhang, *ChemSusChem,* 2013, **6**, 56.

2 P. Lu, Y. Sun, H. Xiang, X. Liang and Y. Yu, *Adv. Energy Mater.,* 2018, **8**, 1702434.

3 B. Cao, H. Liu, B. Xu, Y. Lei, X. Chen and H. Song, *J. Mater. Chem. A,* 2016, **4**, 6472.

4 D. Li, L. Zhang, H. Chen, L. X. Ding, S. Wang and H. Wang, *Chem. Commun.,* 2015, **51**, 16045.

5 H. Liu, M. Jia, N. Sun, B. Cao, R. Chen, Q. Zhu, F. Wu, N. Qiao and B. Xu, *ACS Appl. Mater. Interfaces,* 2015, **7**, 27124.

6 H. Hou, C. E. Banks, M. Jing, Y. Zhang and X. Ji, *Adv. Mater.,* 2015, **27**, 7861.

7 J. Yang, X. Zhou, D. Wu, X. Zhao and Z. Zhou, *Adv. Mater.,* 2017, **29**, 1604108.

8 J. Ding, H. Wang, Z. Li, A. Kohandehghan, K. Cui, Z. Xu, B. Zahiri, X. Tan, E. M. Lotfabad, B. C. Olsen and D. Mitlin, *ACS Nano,* 2013, **7**, 11004.

9 D. Xu, C. Chen, J. Xie, B. Zhang, L. Miao, J. Cai, Y. Huang and L. Zhang, *Adv. Energy Mater.,* 2016, **6**, 1501929.

10 Z. Zhu, F. Cheng, Z. Hu, Z. Niu and J. Chen, *J. Power Sources,* 2015, **293**, 626.

11 B. Yang, S. Liu, X. Guo, H. Song and J. Zhou, *ACS Sustain. Chem. Eng.,* 2018, **6**, 17184-17193.

12 Y.-E. Zhu, L. Yang, X. Zhou, F. Li, J. Wei and Z. Zhou, *J. Mater. Chem. A,* 2017, **5**, 9528.

13 J. Zhang, D.-W. Wang, W. Lv, S. Zhang, Q. Liang, D. Zheng, F. Kang and Q.-H. Yang, *Energy Environ. Sci.,* 2017, **10**, 370.

14 S. Liu, J. Zhou and H. Song, *Small,* 2018, **14**, 1703548.

15 W. Xiao, Q. Sun, J. Liu, B. Xiao, P.-A. Glans, J. Li, R. Li, J. Guo, W. Yang and T.-K. Sham, *Nano Res.,* 2017, **10**, 4378.

16 M. Hu, H. Zhou, X. Gan, L. Yang, Z.-H. Huang, D.-W. Wang, F. Kang and R. Lv, *J. Mater. Chem. A,* 2018, **6**, 1582.

17 X. Guo, X. Zhang, H. Song and J. Zhou, *J. Mater. Chem. A,* 2017, **5**, 21343.

18 H. Kim, J. Hong, Y.-U. Park, J. Kim, I. Hwang and K. Kang, *Adv. Funct. Mater.,* 2015, **25**, 534.

19 Z. Jian, W. Luo and X. Ji, *J. Am. Chem. Soc.,* 2015, **137**, 11566.

20 H. Li, Z. Cheng, Q. Zhang, A. Natan, Y. Yang, D. Cao and H. Zhu, *Nano Lett.,* 2018, **18**, 7407-7413.

21 P. Xiong, X. Zhao and Y. Xu, *ChemSusChem,* 2018, **11**, 202.

22 W. Wang, J. Zhou, Z. Wang, L. Zhao, P. Li, Y. Yang, C. Yang, H. Huang and S. Guo, *Adv. Energy Mater.,* 2018, **8**, 1701648.

23 M. Chen, W. Wang, X. Liang, S. Gong, J. Liu, Q. Wang, S. Guo and H. Yang, *Adv. Energy Mater.,* 2018, **8**, 1800171.

24 Y. An, H. Fei, G. Zeng, L. Ci, B. Xi, S. Xiong and J. Feng, *J. Power Sources,* 2018, **378**, 66.

25 Z. Tai, Q. Zhang, Y. Liu, H. Liu and S. Dou, *Carbon,* 2017, **123**, 54.

26 H. Zhang, H. He, J. Luan, X. Huang, Y. Tang and H. Wang, *J. Mater. Chem. A,* 2018, **6**, 23318-23325.

27 R. Hao, H. Lan, C. Kuang, H. Wang and L. Guo, *Carbon,* 2018, **128**, 224.

28 Z. Jian, Z. Xing, C. Bommier, Z. Li and X. Ji, *Adv. Energy Mater.,* 2016, **6**, 1501874.

29 Z. Jian, S. Hwang, Z. Li, A. S. Hernandez, X. Wang, Z. Xing, D. Su and X. Ji, *Adv. Funct. Mater.,* 2017, **27**, 1700324.

30 K. Share, A. P. Cohn, R. Carter, B. Rogers and C. L. Pint, *ACS Nano,* 2016, **10**, 9738-9744.

31 Y. Xu, C. Zhang, M. Zhou, Q. Fu, C. Zhao, M. Wu and Y. Lei, *Nat. Commun.,* 2018, **9**, 1720.

32 J. Yang, Z. Ju, Y. Jiang, Z. Xing, B. Xi, J. Feng and S. Xiong, *Adv. Mater.,* 2018, **30**, 1700104.

33 D. S. Bin, X. J. Lin, Y. G. Sun, Y. S. Xu, K. Zhang, A. M. Cao and L. J. Wan, *J. Am. Chem. Soc.,* 2018, **140**, 7127.